Fracture Mechanics of Concrete Structures, de Borst et al (eds) © 2001 Swets & Zeitlinger, Lisse, ISBN 90 2651 825 0

Fracture properties of concrete in cryogenic conditions

C.Rocco
Departamento de Construcciones, Facultad de Ingeniería, Universidad Nacional de La Plata, calle 48 y 115, La Plata, CP 1900, Argentina

J.Planas, G.V.Guinea & M.Elices
Dept. Ciencia de Materiales, E.T.S. de Ingenieros de Caminos, Universidad Politécnica de Madrid, Ciudad Universitaria, 28040 Madrid, Spain

ABSTRACT: In this paper, the fracture properties at temperatures ranging from 20 to −170 °C are reported for a concrete mix similar to those used in the walls of liquid natural gas tanks. Stable three-point-bend tests on notched beams, conducted in CMOD control, and standard cylinder-splitting tests were carried out at 20, −20, −70, −120 and −170 °C. From these tests, typical fracture parameters were determined according to the cohesive crack model: tensile strength, fracture energy, softening curve (stress vs. crack opening), characteristic length and modulus of elasticity. The results show that the fracture properties of concrete improve as the temperature is lowered. As the temperature decreases, the tensile strength and the fracture energy increase markedly. From 20 to −170 °C, concrete shows a two-fold increase in tensile strength and a three-fold increase in fracture energy. With regard to the softening curves, the results show that a bilinear approximation is a good estimate even for temperatures as low as −170 °C, and the shape of the curve is very similar for temperatures over −120 °C. A significant difference in the shape, with a much shorter tail, is found at −170 °C. The characteristic length, a measure of the intrinsic brittleness of concrete, is not strongly influenced by the temperature in the range investigated.

1 INTRODUCTION

Concrete structures at low temperatures are currently used for the storage of liquefied gases, barge hulls, floating terminals and drilling hulls. In these applications, temperatures as low as −170 °C can be expected. It is known that standard concrete properties such as compressive strength, tensile strength, rupture modulus and modulus of elasticity can increase markedly at low temperatures. The tests results reported by different authors show that, depending on the water content, the concrete compressive strength at low temperatures can increase up to 400% over that at 20 °C (Elices et al. 1982, The Concrete Society 1982, The Concrete Societies of the Netherlands and the U.K. 1983). The dependence of the tensile strength on temperature, as determined by splitting, bending or double punch tests, is similar to the compressive strength, though less pronounced. The stress-strain response of axially compressed concrete is also influenced by the temperature and moisture content. As the temperature decreases, the compressive stress-strain curve of concrete becomes steeper, more linear and more brittle.

Although the effect of the low temperature on the standard concrete properties, as mentioned above, has long been studied and the results show that at low temperatures the concrete exhibits many desirable features for the design engineer, less is known about the fracture properties of concrete in cryogenic conditions. One question has not been yet answered: is the concrete behavior more brittle at low temperatures? Even though from fracture tests conducted by the authors (Maturana et al. 1990, Elices et al. 1987), it was shown that in saturated concrete the fracture energy is well above that at room temperature, more information is needed to answer this question. In particular, there are no reports on the cohesive crack behavior at low temperatures. In this paper, the fracture properties from 20 to −170 °C of a concrete used to build the prestressed wall of a liquid natural gas tank are reported. Two sets of tests were carried out: a) stable three-point-bend tests on notched beams, conducted in CMOD control, and b) cylinder-splitting tests. The elastic modulus and the bilinear approximation of the curve of stress vs. crack opening (softening curve) were determined at each test temperature. The evolution with temperature of typical fracture parameters associated with the cohesive crack (tensile strength, fracture energy, characteristic length) is also given.

2 MATERIALS AND SPECIMENS

To evaluate the fracture properties of concrete in cryogenic conditions, a typical concrete as used for building land-based storage of liquefied gases was used. To make the concrete, crushed limestone gravel of a nominal maximum size of 20 mm, natural siliceous

sand and ordinary portland cement similar to ASTM type I were used, with three different chemical admixtures: a sodium naphthalene sulfonate type superplasticizer, a non retarder plasticizer, and an air admixture. In mixing, cement, sand and coarse aggregate were dry blended, and water was added with the additives. The cement contents of the mix was 400kg/m^3 and the proportions of the various components are given in Table 1.

Two sets of specimens were prepared and tested: a) cylindrical specimens of 150 mm length and 75 mm diameter for the splitting tensile test, and b) prismatic specimens of 100 x 100 x 470 mm for stable three-point-bend tests. All the specimens were cast from a single batch in steel moulds, compacted on a vibrating table, and immediately stored in a controlled curing chamber at 20 °C and 95% r.h. during 24 hours. Next the specimens were demolded, immediately wrapped in a plastic polyethylene film and coated with paraffin wax to avoid moisture losses and microcracking. In these conditions, the specimens were stored in laboratory environment conditions until the time of the test 60 days later. Just before the three-point-bend test, 50 mm length notches were cut into the specimen thickness on the middle section of the prismatic specimens using a diamond saw. The width of the notches was 2 mm. To measure the specimen temperature during the test, four type K thermocouples were attached to each specimen, two inside the specimen and two on the specimen surface. The inside thermocouples were embedded into the specimen during casting while those on the surface were fixed immediately before the test.

3 EXPERIMENTAL PROCEDURE

To determine the fracture properties of concrete, splitting tensile test and stable three-point-bend tests were performed following procedures similar to ASTM C496, and RILEM TC50 (1985) recommendation respectively. The special features of the procedures are presented below:

Table 1. Mix proportions of concrete (by weight).

cement	water	gravel	sand	SF (%)	P (%)	A (%)
1.0	0.45	2.64	2.28	0.7	1.2	0.07

SF: superplasticizer, P: plasticizer, A: air entraining admx.

3.1 *Low temperature equipment*

To cool the specimens to the test temperature, two low temperature chambers, differing only in volume, were used. The temperature inside the chamber is lowered at a constant rate by spraying a mist of liquid nitrogen controlled by an electromagnetic valve. The intended cooling ramp is input to the temperature controller via a digital function generator, and the feed-back signal is provided by a platinum resistor sensing the gas coolant temperature. The controller automatically operates the electrovalve through a PID control algorithm. The stability of the gas temperature achieved with this system is ±1.5 °C. During cooling, the gas coolant temperature and the temperature of the four type K thermocouples attached to the specimens are continuously recorded via an automatic data acquisition system (DAS). The temperature stability at the specimen measuring points is better than 0.1 °C.

The cooling rates used were 64 °C/hour for splitting test specimens and 32 °C/hour for three-point-bend test specimens. These cooling rates were selected to minimize the thermally induced stress in the specimen bulk, to avoid microcracking and noticeable damage at the notch root (see Maturana et al. 1990 for the details of the determination of the maximum cooling rate).

3.2 *Splitting tensile test*

Tests were performed at 20, −20, −70, −120 and −170 °C, using a 1000 kN servohydraulic universal testing machine Instron 1275 with 8500 digital electronic control. At each temperature, three specimens were tested.

The tests were carried out under displacement control following the ASTM C496 standard recommendation, except that the width of the load-bearing strips was 1/15 of the specimen diameter. The test was run at an actuator displacement rate of 0.15 mm/minute. This rate was selected so that the tensile stress rate in the specimen remained below 1 MPa/minute throughout the test.

Once the test temperature was reached in the specimen, the load was applied continuously until the rupture of the specimen. The bearing strips used to distribute the load on the specimen were of plywood, free of imperfections, 3 mm thick and of 5 mm width. These bearing strips were glued to the specimen in the correct position before the test and were not reused. During the test the load and the temperatures of the thermocouples attached to the specimen were continuously recorded by the automatic data acquisition system.

Table 2. Splitting test results.

Temperature (°C)	N	f_{st} (MPa)	S (MPa)	C_v (%)
+20	3	3.84	0.18	4.8
−20	3	5.30	0.26	4.9
−70	3	6.65	0.79	12.0
−120	3	6.85	0.46	6.7
−170	3	7.11	0.24	3.4

N: Number of tests, f_{st}: splitting tensile strength, S: standard deviation, C_v: coefficient of variation.

3.3 *Stable three-point-bend tests*

Tests were performed at the same temperatures and using the same servohydraulic universal testing machine as that used in the splitting test. At each tem-

perature, three specimens were tested, with a loading span of 400 mm (span-to-depth ratio of 4).

The tests were carried out following a procedure similar to that described in the RILEM TC50 standard recommendations, with the modifications proposed by the authors(Elices et al. 1992; see Bazant & Planas 1998, Sec. 7.3). All the tests were stable, and stability was achieved by running the test in crack mouth opening displacement (CMOD) control. The CMOD rate during the test was 0.03 mm/minute. To measure the CMOD a clip-on gauge MTS 632.03C-51 extensometer with 4.0 mm displacement span was used.

Deflection was measured as the relative displacement of the central loading head relative to the beam supports. Two MTS 63211C-21 extensometers of ± 3.75 mm range were used for this purpose, placed one at each side of the specimen. During the test, the load, the extensometer output signal and the temperatures of the thermocouples attached to the specimen were continuously recorded until complete failure by the automatic data acquisition system.

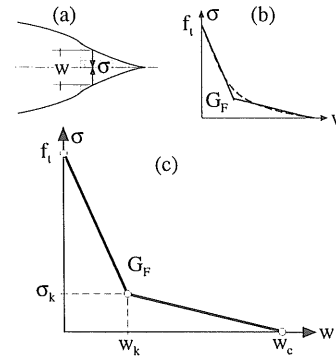

Figure 1. The stress vs. crack opening relationship in a cohesive zone (a) is usually nonlinear as shown by the dashed line in (b). For concrete, a bilinear approximation, shown as a full line in (b), is sufficient in practice to reproduce results within a reasonable accuracy. The softening bilinear curve is fully defined by the four parameters shown in (c).

4 EXPERIMENTAL RESULTS

4.1 *Results of the splitting tensile test*

The main results of the splitting tensile test are summarized in Table 2 which gives the number of tests N, the mean value of the splitting tensile strength f_{st}, the standard deviation S, and the coefficient of variation C_v for each temperature.

4.2 *Results of the three-point-bend tests*

Table 3 summarizes the main results obtained from the three-point-bend test with the number of tests N, the nominal strength σ_{Nu} obtained from equation (1), the energy of fracture G_F , and the elastic modulus E at each temperature. Values in square brackets indicate the standard deviation.

$$\sigma_{Nu} = 6P_u/BD \qquad (1)$$

were P_u is the peak load recorded during the test, B the specimen thickness and D the specimen depth.

Table 3. Three-point-bend tests results.

Temperature (°C)	N	σ_{Nu} (MPa)	G_F (N/m)	E (GPa)
+20	3	1.35 [0.01]	80 [5.5]	39.8
−20	3	2.02 [0.07]	175 [11]	37.6
−70	3	2.56 [0.09]	240 [12]	41.8
−120	3	2.77 [0.19]	271 [27]	46.6
−170	3	2.43 [0.08]	279 [17]	41.6

The elastic modulus was obtained from the initial compliance of the Load-CMOD curve using the expression for the CMOD given by Tada et al. (1985). The energy of fracture was obtained by the procedure described in the RILEM TC50 draft recommendation with the corrections proposed by the authors (Guinea et al. 1992, Planas et al. 1992, Elices et al. 1992; see also Bazant & Planas 1998, Sec 7.3).

4.3 *Parameters of the bilinear softening curve*

From the results of both the splitting test and stable three-point-bend test, the main parameters of the softening function were determined. This function is the relevant material property within the framework of the cohesive crack model used to characterize the fracture behavior of the material. In practice, to determine the softening curve we assumed that it can be appropriately described by a bilinear curve as shown in Figure 1. This hypothesis is usually adopted for concrete. In the figure, the key points of the curve are marked with an open symbol. A complete description of the method used to fit the bilinear curve parameters, i.e. "the general bilinear fit method for the softening curve of concrete", is given in Guinea et al. (1994) and also in Bazant & Planas (1998), Sec. 7.3.

Table 4. Parameters of the bilinear softening curves.

Temperature (°C)	f_t (MPa)	w_k (μm)	σ_k (MPa)	w_c (μ m)	ℓ_{ch} (mm)
+20	3.84	19	0.43	201	216
−20	5.30	40	0.48	314	234
−70	6.65	41	0.77	281	226
−120	6.85	47	0.82	337	269
−170	7.11	22	2.00	198	229

Table 4 indicates the parameters of the softening curves obtained at each test temperature. It includes the tensile strength f_t, the coordinates, σ_k and w_k, of the curve break-point, and the critical crack opening, w_c. Note that the value of the splitting tensile strength

was assumed as a true value of the tensile strength. In a recent in-depth study of the splitting test the authors demonstrated that for the specimen size and width of the bearing strips used in the present tests, this assumption is accurate (Rocco et al. 1999a,b).

In Table 4, the characteristic length ℓ_{ch} calculated from equation (2) is also included. In the context of the cohesive crack model, ℓ_{ch} is a fracture parameter used to describe the intrinsic brittleness of the material.

$$\ell_{ch} = EG_F/f_t^2 \qquad (2)$$

5 DISCUSSION AND FINAL REMARKS

5.1 *Influence of low temperatures on splitting tensile strength and fracture energy*

Figure 2 shows the evolution of the splitting tensile strength with the temperature. The error bars correspond to ± the standard deviation. The experimental results show that the splitting tensile strength of concrete at low temperature displays a noticeable increment, especially from 20 to −70 °C. Below −70 °C the influence of the temperature on the tensile strength becomes less pronounced and the strength values seem to approach an asymptotic value. These results are qualitatively similar to those found by Maturana et al. (1990) for a concrete with siliceous aggregates and cured and stored immersed in lime saturated water. However, the increase in strength is qualitatively much greater in the present concrete as the bottom diagram in Figure 2 shows.

Figure 3 shows the evolution of the fracture energy with the temperature. The error bars correspond to ± the standard deviation. As shown in the figure, the fracture energy of concrete increases as the temperature decreases but seems to approach an asymptote at temperatures below −120 °C. When these results are compared with those of Maturana et al. (1990) as shown in the diagram in the bottom of Figure 3, one finds that the results are remarkably similar, to the extent that the relative evolution of G_F is coincident within experimental scatter.

The increase of the splitting tensile strength and the fracture energy at low temperatures can be explained by the freezing of water in the bulk of the concrete. During cooling, the free water trapped in the complex network of capillary pores of the hardened cement paste solidify, gradually sealing the pores and strengthening the material. However, this is only a qualitative explanation, and further basic research is needed to understand the complex thermodynamic phenomena taking place during cooling.

5.2 *Influence of low temperature on the softening curve*

Figure 4 shows, for each test temperature, the softening curves of concrete obtained from the results included in Table 4. Note that from 20 to −120 °C, the softening curves are similar, in that the slopes of the two linear segments are close to each other. Between −120 and −170 °C the softening curve changes abruptly. At −170 °C the initial slope of the curve becomes steeper and the tail of the curve shorter.

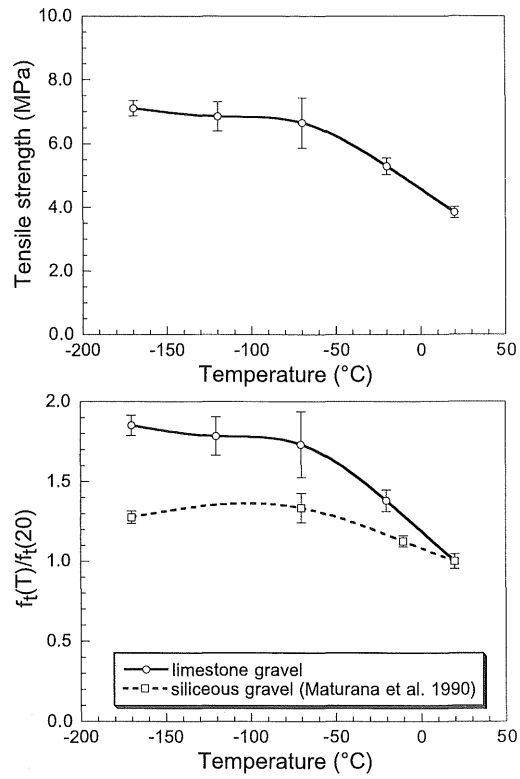

Figure 2. Effect of low temperatures on the splitting tensile strength: absolute values (top), and comparison of values relative to that at 20 °C with the results of Maturana et al. (bottom).

The similitudes and differences of the softening curves become more evident when these curves are plotted nondimensionally by dividing the tensile stress by the tensile strength and the crack opening by the fracture energy to tensile strength ratio (G_F/f_t). The dimensionless softening curves obtained in this way are shown in Figure 5. Note that except at −170 °C, the shapes of the curves are very close to each other.

Finally, Figure 6 shows the evolution of the characteristic length ℓ_{ch} with the temperature. It is worth remembering that if both the shape of the softening curve and the size of the structure are held constant, the brittleness of the structure may be measured by the

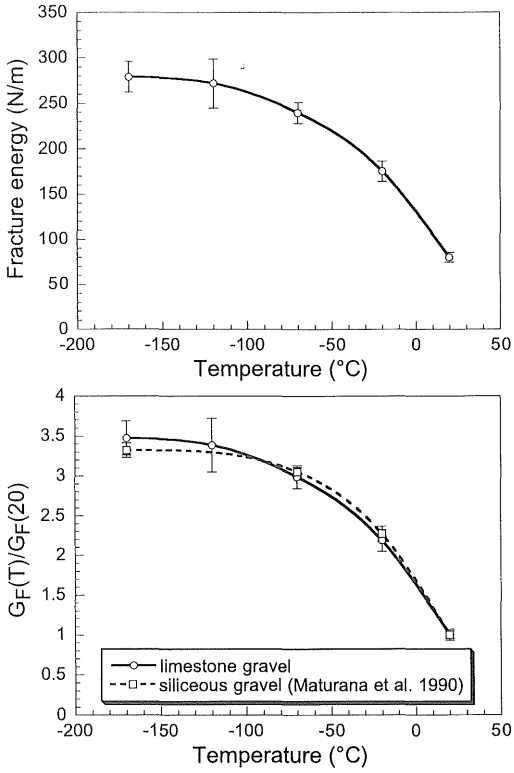

Figure 3. Effect of low temperatures on the fracture energy: absolute values (top), and comparison of values relative to that at 20 °C with the results of Maturana et al. (bottom).

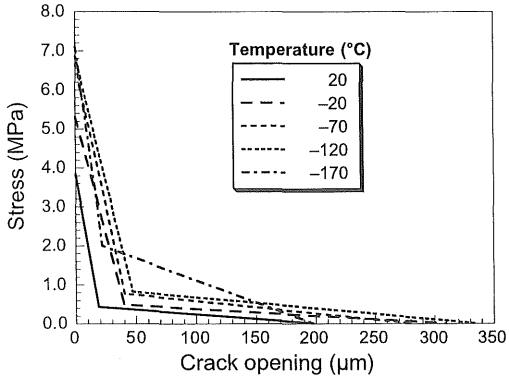

Figure 4. Softening curve of concrete at various temperatures.

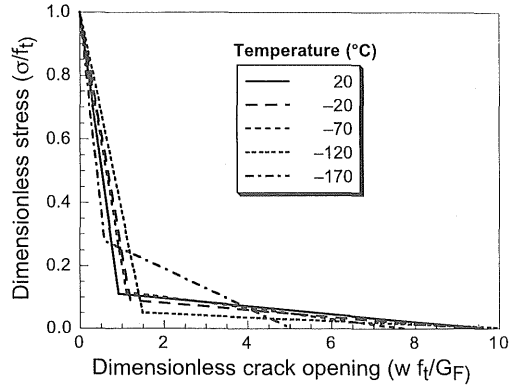

Figure 5. Dimensionless softening curve of concrete at different temperatures.

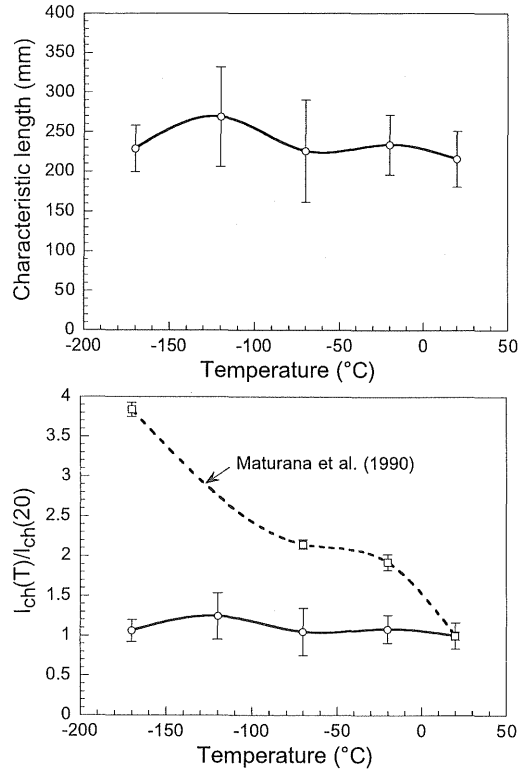

Figure 6. Evolution of the characteristic length with temperature: absolute values (top), and comparison of values relative to that at 20 °C with the results of Maturana et al. (bottom).

inverse of the characteristic length. The results in Figure 6, show that ℓ_{ch} remains approximately constant or increases slightly at low temperatures. This indicates that lowering the temperature does not increase the brittleness of concrete. The results found by Maturana et al. for the water-saturated, siliceous gravel concrete was much more optimistic, in that the brittleness decreased (ℓ_{ch} increased) by a factor of 4. The difference between the two sets of results is shown in the diagram in the bottom of Figure 6. The reason for the different trend in the brittleness is mainly due to the different quantitative trend in the tensile strength (see fig. 2). Since ℓ_{ch} increases with G_F and decreases with f_t *squared*, the relative influence of f_t is much higher.

The main practical conclusion is that, for the concrete tested in this work, even though the tensile strength, the modulus of elasticity and the energy of fracture all increase strongly at low temperatures, the characteristic length (i.e., the brittleness) and the shape of the softening curve remain similar down to −170 and −120 °C, respectively. An abrupt change is observed in the shape of the softening curve at −170 °C, an effect that deserves further research.

REFERENCES

Bazant, Z.P. & Planas, J. 1998. *Fracture and Size Effect in concrete and other Quasibrittle Materials.* Boca Raton: CRC Press.

The Concrete Society 1982. *Cryogenic Concrete.* Construction Press.

The Concrete Societies of the Netherlands and the U.K. 1983.*Cryogenic Concrete.* Concrete Society.

Elices, M., Guinea, G.V. & Planas, J. 1992. Measurement of the fracture energy using three-point bend tests: 3. Influence of cutting the P-δ tail. *Materials and Structures* **25**, 327–334.

Elices, M., Planas, J. & Maturana, P. 1987. Fracture of concrete at cryogenic temperatures. In S.P. Shah & S.E. Swartz (eds.), *Fracture of Concrete and Rock*: 159–169. Bethel, CT, USA: SEM (Society for Experimental Mechanics).

Elices, M., Rostasy, F. S., Faas, W. M. & Wiedemann, G. 1982. *Cryogenic behavior of materials for prestressed concrete.* FIP State of the Art Report. Wexham Springs: FIP.

Guinea, G.V., Planas, J. & Elices, M. 1992. Measurement of the fracture energy using three-point bend tests: 1. Influence of experimental procedures. *Materials and Structures* **25**, 212–218.

Guinea, G.V. Planas, J. & Elices, M. 1994. A general bilinear fit for the softening curve of concrete *Materials and Structures* **27**, 99–105.

Maturana, P., Planas, J. & Elices, M. 1990. Evolution of fracture behavior of saturated concrete in the low temperature range. *Engineering Fracture Mechanics* **35**, 827–834.

Planas, J., Elices, M., & Guinea, G.V. 1992. Measurement of the fracture energy using three-point bend tests: 2. Influence of bulk energy dissipation. *Materials and Structures* **25**, 305–312.

RILEM 1985. Determination of the fracture energy of mortar and concrete by means of three-point bend tests on notched beams. *Materials and Structures* **18**, 285–290. (RILEM Draft Recommendation, TC 50-FMC Fracture Mechanics of Concrete.)

Rocco, C., Guinea, G.V., Planas, J. & Elices, M. 1999a. Size effect and boundary conditions in the Brazilian test: experimental verification. *Materials and Structures* **32**: 210–217.

Rocco, C., Guinea, G.V., Planas, J. & Elices, M. 1999b. Size effect and boundary conditions in the Brazilian test: theoretical analysis. *Materials and Structures* **32**: 437–444.

Tada, H., Paris, P. & Irwin, G. 1985. *The Stress Analysis of Cracks Handbook.* St Louis, Missouri: Del Research Corporation.